Inorg. Chem. **2002**, *41*, 76–85

Synthesis and Structural Characterization of the $\{[Rh_5(CO)_{14}]–(H_2N(CH_2)_4NH_2)–[Rh_5(CO)_{14}]\}^{2-}$ and $[Rh_5(CO)_{13}(H_2N(CH_2)_2NH_2)]^-$ Anions (as $[PPh_4]^+$ Salts): An Unprecedented Example of Carbonyl Substitution by Alkylamines in a Homoleptic Metal Carbonyl Cluster Anion

Alessandro Fumagalli,*,† Maria Carlotta Malatesta,‡ Anna Tentori,‡ Diego Monti,§ Piero Macchi,|| and Angelo Sironi*,||

Dipartimento di Biologia Strutturale e Funzionale dell'Università dell'Insubria, Via J. H. Dunant 3, 21100 Varese, Italy, Dipartimento di Chimica Inorganica, Metallorganica e Analitica and Dipartimento di Chimica Strutturale e Stereochimica Inorganica, Università di Milano, Via G. Venezian 21, 20133 Milano, Italy, and Centro di Studio CNR sulle Sostanze Organiche Naturali, Via G. Venezian 21, 20133 Milano, Italy.

Received July 26, 2001

The substitution of one or two carbonyls by many different primary and secondary alkylamines and -diamines has been established for the first time in a homoleptic carbonyl cluster anion, the trigonal bipyramidal $[Rh_5(CO)_{15}]^-$. Two derivatives, the bis-monosubstituted $\{[Rh_5(CO)_{14}]–(H_2N(CH_2)_4NH_2)–[Rh_5(CO)_{14}]\}^{2-}$ dianion (**1**) and the disubstituted chelated $[Rh_5(CO)_{13}(H_2N(CH_2)_2NH_2)]^-$ monoanion (**2**), have been structurally characterized, both in the solid state (as $[PPh_4]^+$ salts) and in solution, revealing that the sites of the substitution are the cluster apexes. ^{13}C NMR spectra of **2** revealed localized fluxionality of the CO ligands over the temperature range 298–183 K.

Introduction

Carbonyl substitution at one or several metal sites of a metal carbonyl cluster is a well-known reaction, and large numbers of compounds have been produced with a wide variety of ligands.[1] However, literature reports concerning reactions of neutral or anionic metal carbonyl clusters, with aliphatic amines or ammonia, formally replacing one CO ligand are, to date, quite scarce. To our knowledge, there is only one report where a 50-electron Os_3 cluster yields an ethylamine adduct, with loss of a CO group and concomitant displacement of one η^2-bound acetylide.[2] In the few other reported cases, the amino derivatives have been obtained by addition rather than by substitution and essentially with electron-deficient metal clusters of the d^8 group.[3,4] The reason for such a scarcity of CO-substitution reactions with aliphatic amines or ammonia is quite simple: the high electron density on the cluster metal atoms opposes the substitution of the π-acid CO with a nitrogen ligand that is capable of essentially σ-bonding without the possibility for metal back-donation. Consequently, treatment of a metal carbonyl cluster with an amine usually leads to its reduction instead of CO substitution, as observed for other bases such as OH^- or RO^-. Many years ago, P. Chini and S. Martinengo[5] suggested that nucleophilic attack on a carbonylic carbon might be the first common step for many reactions, even those that eventually result in CO substitution, as in the case of halides or pseudohalides. Thus, $Rh_6(CO)_{16}$ was shown to give a carbamoyl derivative by reaction with a primary amine (and assistance

* To whom correspondence should be addressed. Phone: +39 0332 421548. Fax: +39 0332 421554. E-mail: alessandro.fumagalli@uninsubria.it. For structural characterization, E-mail: angelo@csmtbo.mi.cnr.it.

† Università dell'Insubria.

‡ Dipartimento di Chimica Inorganica, Università di Milano.

§ Centro di Studio CNR sulle Sostanze Organiche Naturali.

|| Dipartimento di Chimica Strutturale e Stereochimica Inorganica, Università di Milano.

(1) Darensbourg, D. J. In *The Chemistry of Metal Cluster Complexes*; Shriver, D. F., Kaesz, H. D., Adams, R. D., Eds.; VCH Publishers: New York, 1990; p 171.

(2) Cherkas, A. A.; Taylor, N. J.; Carty, A. J. *J. Chem. Soc., Chem. Commun.* **1990**, 385.

(3) Adams, R. D.; Wang, S. *Inorg. Chem.* **1986**, *25*, 2534.

(4) Bar Din, A.; Bergman, B.; Rosenberg, E.; Smith, R.; Dastrù, W.; Gobetto, R.; Milone, L.; Viale, A. *Polyhedron* **1998**, *17*, 2975.

(5) Chini, P.; Martinengo, S.; Giordano, G. *Gazz. Chim. Ital.* **1972**, *102*, 330.

10.1021/ic0107936 CCC: $22.00 © 2002 American Chemical Society
Published on Web 12/14/2001

Table 1. IR CO Stretching (± 2 cm^{-1}) of the Apical Monosubstituted $[Rh_5(CO)_{14}(n)]^-$ Derivatives in THF under 1 atm of CO[a]

n	terminal COs				bridging COs			
bzn^S	2063 w	2035 s	2017 m	1990 s	1872 ww	1835 ms	1772 m	
Ph-pn^S	2062 w	2034 s	2014 m	1989 s	1871 ww	1835 ms	1771 m	
piperidine^S	2062 w	2035 s	2016 m	1990 s	1869 ww	1833 ms	1771 ms	
cad^S	2062 w	2034 s	2015 m	1987 s		1834 ms	1771 ms	
put^{S,M}	2062 w	2035 s	2015 m	1988 s	1876 ww	1834 ms	1772 ms	
put^C (Nujol mull)	2071 w	2039−30 m		1985 s	1872 w	1830−17 m	1778−68 m	1728 m
$[Rh_5(CO)_{14}PPh_3]^-$ [13]	2061 w	2036 s		1994 vs		1832 ms	1775 m	

[a] In units of cm^{-1}. n = benzylamine (bzn), 3-phenylpropylamine (Ph-pn), 1,4 diaminobutane (put), 1,5-diaminopentane (cad). The superscripts have the following meaning: (S) PPN^+ salt obtained in solution at ca. 1:1 molar ratio, if not otherwise specified; (M) in mixture with the chelated form within the range (1.0−2.5):1.0 of molar ratios; the IR spectrum has been obtained by spectral subtraction (see Figure 1S in the Supporting Information); (C) crystalline $[PPh_4]^+$ salt of $[Rh_5(CO)_{14}-(put)-Rh_5(CO)_{14}]^{2-}$.

of a second amine molecule):

$$Rh_6(CO)_{16} + 2RNH_2 \rightarrow [Rh_6(CO)_{15}C(O)NHR]^- + [RNH_3]^+ \quad (1)$$

This product is somewhat stable only under anhydrous conditions and in the presence of trace amounts of water decomposes. The result is a reduction with production of a cluster anion:

$$[Rh_6(CO)_{15}CONHR]^- + H_2O \rightarrow [Rh_6(CO)_{15}]^{2-} + CO_2 + [RNH_3]^+ \quad (2)$$

Of course, the $[Rh_6(CO)_{15}]^{2-}$ dianion[6] is less sensitive to further reduction than the parent neutral species because of further buildup of negative charge, and at higher concentrations of amine (or a generic base) only, it can give $[Rh_7(CO)_{16}]^{3-}$.[6,7] This reactivity with amines has been reproduced for several rhodium carbonyl clusters, both neutral and anionic; with the less reduced species we eventually observed only reduction reactions that very likely were induced by traces of water with the carbamoyl intermediate. Highly reduced species are unreactive.

The present report deals with the highly unusual reactivity of the $[Rh_5(CO)_{15}]^-$ monoanion,[8] which gives substitutions of one or two carbonyls with alkylamines. This pentanuclear cluster is quite peculiar in that it exists only in the presence of CO. Its involvement in the catalytic synthesis of ethylene glycol and its persistence at high pressures of CO/H_2, (1−2 kbar), were also demonstrated;[9,10] our new finding presented herein may add further insight to the amine-promoted catalytic reactions.[11]

Result and Discussion

1. Single CO Substitution on the $[Rh_5(CO)_{15}]^-$ Anion by a Primary or Secondary Amine. The $[Rh_5(CO)_{15}]^-$ anion (as $[PPN]^+$ or $[PPh_4]^+$ salt)[12] readily reacts in THF or acetone solution with benzylamine (bzn), 3-phenylpropylamine (Ph-pn), or piperidine (NHC_5H_{10}, a cyclic secondary amine); a sudden change of color, from burgundy-red to orange, and conspicuous gas evolution is observed. One apical carbonyl of the trigonal bipyramidal Rh_5 cluster undergoes substitution by the amine. This takes place according to eq 3 (here exemplified with a primary amine), despite the CO atmosphere that is required for the stabilization of the Rh_5 substrate:[8]

$$[Rh_5(CO)_{15}]^- + NH_2R \xrightarrow{CO\ (1\ atm)} [Rh_5(CO)_{14}(NH_2R)]^- + CO \quad (3)$$

Excess amounts of amine (up to 3 times) did not give evidence of any further reaction. The substitution products are fairly stable in solution, even under a nitrogen atmosphere (a few hours) and, unlike the above-mentioned carbamoyl derivatives, are not sensitive to water up to a concentration of several percent.

Solution IR spectra of all the derivatives of this group are almost identical in the carbonyl-stretching region. As evidenced in Table 1, these spectra compare well with that of the $[Rh_5(CO)_{14}(PPh_3)]^-$ [13] anion where CO substitution occurs analogously in the apical position of the trigonal bipyramidal Rh_5 cluster.

Diamines with a rather long spacer such as 1,4-diaminobutane (putrescine, put) and 1,5-diaminopentane (cadaverine, cad), can act as bis-unidentate ligands, at least when the reaction is done under 1 atm of CO. This is exemplified by the chained $[Rh_5(CO)_{14}-put-Rh_5(CO)_{14}]^{2-}$ dianion (**1**), which was isolated and structurally characterized (Figure 1). At this point, we must also anticipate the possibility of diamines of undergoing chelation: this linkage is evidenced from IR spectra in solution, in the case of putrescine. Thus, under 1 atm of CO and put/$[Rh_5(CO)_{15}]^-$ molar ratios ranging between 0.6:1 and 1:1, we could detect, together with **1**, minor amounts of the chelated product $[Rh_5(CO)_{13}(put)]^-$ (estimated 5−20%) and even some unreacted $[Rh_5(CO)_{15}]^-$.

(6) Martinengo, S.; Chini, P. *Gazz. Chim. Ital*. **1972**, *102*, 344.
(7) This is the first observable product that can be obtained by reduction of $[Rh_6(CO)_{15}]^{2-}$. Further details of the reductive process of rhodium carbonyl cluster anions: Fumagalli, A. *Mater. Chem. Phys.* **1991**, *29*, 211−220.
(8) Fumagalli, A.; Koetzle, T. F.; Takusagawa, F.; Chini, P.; Martinengo, S.; Heaton B. T. *J. Am. Chem. Soc.* **1980**, *102*, 1740 and references therein.
(9) Heaton, B. T.; Strona, L.; Jonas, J.; Eguchi, T.; Hoffman, G. A. *J. Chem. Soc., Dalton Trans.* **1982**, 1159.
(10) Röper, M.; Schieren, M.; Fumagalli, A. *J. Mol. Catal.* **1986**, *34*, 173 and references therein.
(11) Doyama, T. J. K.; Onitsuka, K.; Shioara, T.; Takahashi, S. *Organometallics* **1991**, *10*, 2493
(12) Availability of $[Rh_5(CO)_{15}]^-$ is generally restricted to the $[PPN]^+$ salt (as a crystalline solid) and the $[PPh_4]^+$ salt (in solution only, see Experimental Section). To our knowledge, any attempt made to precipitate $[Rh_5(CO)_{15}]^-$ with any cation $[Cat]^+$ but $[PPN]^+$ invariably yielded $[Cat]_2[Rh_{12}(CO)_{30}]$.
(13) Fumagalli, A.; Martinengo, S.; Galli, D.; Allevi, C.; Ciani, G.; Sironi, A. *Inorg. Chem.* **1990**, *29*, 1408.

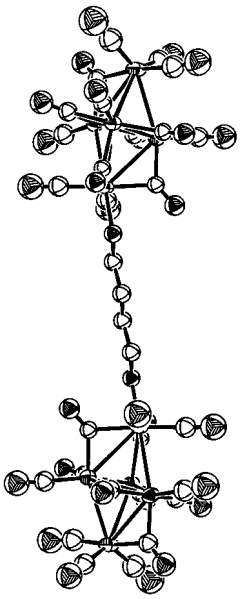

Figure 1. View of the $[Rh_5(CO)_{14}-(put)-Rh_5(CO)_{14}]^{2-}$ dianion (**1**), which has a crystallographically imposed C_i symmetry. Atom labels for the asymmetric part are reported in Figure 2. Atoms are idealized with spheres (Rh and O atoms are shaded).

At higher molar ratios, $[Rh_5(CO)_{15}]^-$ is virtually absent, and the chelation grows to prevail over the unidentate binding (see later).

Dianion **1** was isolated, with quantities of putrescine ranging between 0.6 and 1.6 mol per mole of $[Rh_5(CO)_{15}]^-$, by precipitation of its $[PPh_4]^+$ salt. The crystalline product, redissolved in THF under CO, yielded essentially the same IR spectrum of the unidentate compound in a mixture possessing minor amounts of the chelate and some "free" $[Rh_5(CO)_{15}]^-$. The IR bands of the "pure" product in solution given in Table 1 have been obtained by spectral subtraction as described in the following section.

These monosubstituted $[Rh_5(CO)_{14}(n)]^-$ derivatives, though indefinitely stable in solution under CO, gave decomposition during various attempts of isolation by precipitation. Thus, none but the chained $[Rh_5(CO)_{14}-(put)-Rh_5(CO)_{14}]^{2-}$ dianion was actually isolated in the solid state.

No evidence of any reaction was observed either with a bulky secondary amine, $NH(n\text{-}C_8H_{17})_2$, or with the tertiary amines Me_3N and quinuclidine (a rigid bicycloamine) constantly under CO atmosphere. This unreactivity, which is in direct contrast with the positive response of piperidine (a cyclic secondary amine), is attributed to the steric impediment of the two long (or three) aliphatic chains. On the other hand, the lack of reactivity of *p*-toluidine and diphenylamine may be rationalized in terms of the lower basicity of the two aromatic amines relative to these of the aliphatic ones.

2. Double CO Substitution on the $[Rh_5(CO)_{15}]^-$ Anion by a Chelating Diamine. The reaction of $[Rh_5(CO)_{15}]^-$ with stoichiometric amounts of ethylenediamine (en), (*R*)-(+)-1,2-diaminopropane (*R*-1,2prn) or 1,3-diaminopropane (1,3pm) is, according to IR spectra, apparently quantitative. The chelation, which implies a double CO substitution on an apical rhodium atom, produces five- or six-membered rings, even under a CO atmosphere (0.5−1 atm). For a generic bidentate nitrogen ligand n_2 the simple stoichiometry is

$$[Rh_5(CO)_{15}]^- + n_2 \xrightarrow{CO} [Rh_5(CO)_{13}(n_2)]^- + 2CO \quad (4)$$

All of these derivatives in solution show the same IR spectrum in the carbonyl-stretching region with the characteristic bands given in Table 2. The band-shift to lower wavenumbers (30−15 cm^{-1}) with respect to the monosubstituted derivatives is consistent with an increase in back-donation arising from a reduced number of carbonyls.

As mentioned above, the products from reactions with 1,4 diaminobutane (putrescine, put) appear to be evenly divided between the unidentate and the chelated binding modes. Under CO atmosphere (1 atm) and with an excess of diamine (2.5:1.0), the chelated form slightly prevails (estimated 55%) over the unidentate one. Switching to a nitrogen atmosphere, a condition favoring the substitution of a second carbonyl ligand, shifts the equilibrium (eq 4) toward the chelated form. As indicated by IR (Table 2) the reaction is apparently quantitative. Spectral subtraction gave the carbonyl band pattern for the "pure" unidentate form reported in Table 1. As mentioned earlier, cadaverine gave IR evidence of essentially unidentate binding under a CO atmosphere. Under nitrogen, even cadaverine switches to the chelated form (Table 2). The stability of the eight-membered ring is therefore so low that it cannot exist in CO atmosphere. A few attempts were done to isolate the chelate derivatives of both cadaverine and putrescine. Unfortunately, after a long crystallization process (ca. a week) under a N_2 atmosphere, only amorphous impure products were obtained. Upon further manipulation, these products eventually decomposed to $[Rh_{12}(CO)_{30}]^{2-}$.[14]

In direct contrast, the ethylenediamine derivative $[Rh_5(CO)_{13}(en)]^-$ (**2**) is such a stable molecule that it is generated even from $[Rh_{12}(CO)_{30}]^{2-}$ or $[Rh_6(CO)_{15}]^{2-}$ via a disproportionation reaction, which implies a fragmentation of the metal skeleton. The reaction of the hexanuclear dianion with ethylenediamine under CO goes neatly, with tetracarbonylrhodate as the only byproduct (IR band at 1897 cm^{-1}), thus suggesting the simple relation

$$[Rh_6(CO)_{15}]^{2-} + en \xrightarrow{CO} [Rh_5(CO)_{13}(en)]^- + [Rh(CO)_4]^- \quad (5)$$

The highly reduced $[Rh_7(CO)_{16}]^{3-}$ anion is unreactive in this respect.

Remarkably, the $[Rh_5(CO)_{13}(n_2)]^-$ anions are moderately stable in the absence of CO, differing in this respect from the $[Rh_5(CO)_{15}]^-$ precursor. $[PPh_4][Rh_5(CO)_{13}(en)]$ in THF solution undergoes a change of color, from orange to brown, only after several hours in a continuously renewed static vacuum. Minor changes were observed even in the IR spectra, indicating partial decomposition. Restoring a CO atmosphere causes reaction back to the original product.

(14) Chini, P.; Martinengo, S. *Inorg. Chim. Acta* **1969**, *3*, 299.

Table 2. IR CO Stretching (± 2 cm^{-1}) of the Apical Chelated Derivatives $[Rh_5(CO)_{13}(n_2)]^-$ in THF under 1 atm of CO (Where Not Specified N_2)[a]

n_2	terminal COs			bridging COs				
Apical Chelation								
en[C b]	2034 m	2004 ms	1975 s	1864 ww	1823 m	1809 mw	1775 sh	1754mw
R-1,2prn[C c]	2034 m	2004 ms	1976 s	1864 ww	1822 m	1810 mw	1775 sh	1753mw
1,3prn[C c]	2035 m	2004 ms	1978 s	1867 ww	1825 m	1810 mw	1773 ww	1749mw
put[S b] (2.5:1.0, N_2)	2036 m	2004 ms	1979 s	1865 ww	1824 m	1805 mw	1776 ww	1753mw
cad[S c] (N_2)	2035 m	2003 ms	1979 s	1865 ww	1824 m	1805 mw	1775 ww	1754mw
Further CO Substitution								
en[S b] (N_2)	2019 m	1968 s	1851 ww	1805 m	1789 mw	1733 mw		
1,3prn[S c] (N_2)		2019 w	1968 s	1851 m	(by subtraction of some monochelated form)			

[a] In units of cm^{-1}. [b] PPh_4^+ salt. [c] PPN^+ salt. n_2 = ethylenediamine (en), 1,3-diaminopropane (1,3prn), *R*-(+)-1,2-diaminopropane (*R*-1,2prn), 1,4-diaminobutane (put), 1,5-diaminopentane (cad). The roman superscripts have the following meaning: (S) obtained only in solution, at ca. 1:1 molar ratio if not otherwise specified; (C) crystalline or isolated as a solid.

Evidence of further CO substitution, possibly chelation on both apexes of the Rh_5 cluster, was obtained only with en and 1,3-diaminopropane (Table 2). A nitrogen atmosphere and a strong excess of chelating diamines are required to force this reaction, which is apparently complete only with en. In the second case, the monochelated form still persists. This is consistent with CO being competitive only in the second step of substitution:

$$[Rh_5(CO)_{15}]^- \xrightarrow{CO,\ en} [Rh_5(CO)_{13}(en)]^- \underset{CO}{\overset{N_2,\ en}{\rightleftharpoons}} [Rh_5(CO)_{11}(en)]^- \quad (6)$$

The products are rather unstable and decompose within a few days, thus preventing any attempts of recovery.

In a report concerning the synthesis and characterization of $[Rh_5(CO)_{13}(py)_2]^-$, the possible formation of $[Rh_5(CO)_{13}(en)]^-$ was also suggested on the basis of an interpretation of IR spectra.[15] This reaction was reported as a disproportionation induced by pyridine (or possibly en) of the neutral carbonyls, $Rh_4(CO)_{12}$ or $Rh_6(CO)_{16}$, along with concomitant production of a Rh(I) derivative:

$$3Rh_4(CO)_{12} \xrightarrow{py} 2\ cis\text{-}[Rh(CO)_2(py)_2]^+ + 2[Rh_5(CO)_{13}(py)_2]^- + 6CO \quad (7)$$

This reaction is similar to those induced by halides,[13] which we demonstrated as occurring in two distinct steps. The first step consists of a disproportionation reaction, according to the stoichiometry

$$3Rh_4(CO)_{12} + 4X^- \rightarrow 2[Rh_5(CO)_{15}]^- + 2[Rh(CO)_2X_2]^- + 2CO \quad (8)$$

The second step, which involves carbonyl replacement by X^- in the pentanuclear rhodium cluster, is independent and also occurs with other nucleophiles (such as SCN^- or PPh_3):

$$[Rh_5(CO)_{15}]^- + X^- \rightarrow [Rh_5(CO)_{14}X]^{2-} + CO \quad (9)$$

This two-step sequence very likely applies to the production of the pyridine derivative too.

3. Crystal Structures of $[PPh_4]_2[Rh_5(CO)_{14}-(put)-Rh_5(CO)_{14}]$ and $[PPh_4][Rh_5(CO)_{13}(en)]\cdot THF$. The $[Rh_5(CO)_{14}-(put)-Rh_5(CO)_{14}]^{2-}$ anions in the crystal structure of the $[PPh_4]^+$ salt are hosted within columnar cavities, with a rectangular base and parallel to the short *b* axis (9.83 Å). These channels are generated by the rectangular assembling of the principal cation packing motif; i.e., double columns are interconnected by facing phenyl rings (one for each $[PPh_4]^+$ cation). The $[Rh_5(CO)_{13}(en)]^-$ anions in the crystal structure of the $[PPh_4]^+$ salt pack in columns parallel to the actual *b* axis, but in this structure clathrated THF molecules are hosted between anion and cation columns. Selected bond distances and angles for the two anions are given in Table 3.

The $[Rh_5(CO)_{14}-(put)-Rh_5(CO)_{14}]^{2-}$ anion (**1**) (Figure 1) lies about a crystallographic inversion center bisecting the central C−C bond of the putrescine ligand. The overall stereochemistry is rather uncommon because of the coupling of two metal cages by means of the putrescine ligand, which has an elongated all-trans conformation. In contrast, the ethylenediamine ligand acts as a chelating ligand in **2** and has an envelope conformation. The trigonal bipyramidal Rh_5 units in $Rh_5(CO)_{14}L$ (**1**) and $Rh_5(CO)_{13}L_2$ (**2**) (Figure 2) are elongated in the direction of an ideal 3-fold axis (which is typical for trigonal bipyramidal clusters containing 76 CVE) and have the same ligand stereochemistry as that of the $[Rh_4M(CO)_{15}]^{2-}$ anions (M = Fe, Ru, Os)[17] rather than that of the parent $[Rh_5(CO)_{15}]^-$ anion. Indeed, there are nine terminally bonded ligands, one for each of the three equatorial metals and three on each apical metal. Of the six edge-bridging carbonyls, three are located in almost coplanar positions on the equatorial triangle edges. Two others connect the substituted apical Rh with two of the equatorial metals (Rh2 and Rh4), while the sixth one connects the remaining equatorial Rh with the unsubstituted Rh atom. As is usually observed and theoretically predicted,[16] nucleophilic ligand substitution in the C_2 symmetric $[Rh_5(CO)_{15}]^-$ species preferentially occurs at the apical site and, upon substitution, the overall ligand envelope rearranges to afford the above-described C_s symmetric stereochemistry.

(15) Fachinetti, G.; Funaioli, T.; Zanazzi, P. F. *J. Organomet. Chem.* **1993**, *460*, C34−C36.

(16) Macchi, P.; Proserpio, D. M.; Sironi, A. *Organometallics* **1997**, *16*, 2101−2109.

(17) Fumagalli, A.; Garlaschelli, L.; Della Pergola, R. *J. Organomet. Chem.* **1989**, *362*, 197.

Table 3. Bond Lengths (Å) and Angles (deg) within Anions **1** and **2**[a]

anion **1**		anion **2**		anion **1**		anion **2**	
Rh(1)−Rh(2)	2.9949(6)	Rh(1)−Rh(2)	2.9892(4)	C(23B)−O(23B)	1.143(6)	C(23B)−O(23B)	1.163(3)
Rh(1)−Rh(3)	2.9476(6)	Rh(1)−Rh(3)	2.9360(4)	C(24B)−O(24B)	1.158(5)	C(24B)−O(24B)	1.172(3)
Rh(1)−Rh(4)	2.9787(6)	Rh(1)−Rh(4)	2.9123(5)	C(34B)−O(34B)	1.164(6)	C(34B)−O(34B)	1.157(3)
Rh(2)−Rh(3)	2.7190(6)	Rh(2)−Rh(3)	2.7047(4)	C(35B)−O(35B)	1.172(6)	C(35B)−O(35B)	1.177(3)
Rh(2)−Rh(4)	2.6890(6)	Rh(2)−Rh(4)	2.6822(6)	N−C(1N)	1.469(6)	N(1)−C(1N)	1.456(4)
Rh(2)−Rh(5)	3.0396(7)	Rh(2)−Rh(5)	3.0513(5)			N(2)−C(2N)	1.464(4)
Rh(3)−Rh(4)	2.7364(6)	Rh(3)−Rh(4)	2.7295(6)	C(1N)−C(2N)	1.505(6)	C(1N)−C(2N)	1.456(4)
Rh(3)−Rh(5)	2.9294(6)	Rh(3)−Rh(5)	2.9565(5)	C(2N)−C(2N)#1	1.518(9)		
Rh(4)−Rh(5)	2.9872(6)	Rh(4)−Rh(5)	2.9687(5)	O(11)−C(11)−Rh(1)	177.8(6)	O(1)−C(1)−Rh(1)	173.1(2)
Rh(1)−N	2.190(4)	Rh(1)−N(1)	2.177(2)	O(12)−C(12)−Rh(1)	176.6(6)		
Rh(1)−C(11)	1.953(6)	Rh(1)−N(2)	2.222(2)	O(2)−C(2)−Rh(2)	179.3(5)	O(2)−C(2)−Rh(2)	179.6(3)
Rh(1)−C(12)	1.955(6)	Rh(1)−C(1)	1.934(3)	O(3)−C(3)−Rh(3)	177.7(6)	O(3)−C(3)−Rh(3)	177.5(3)
Rh(2)−C(2)	1.872(5)	Rh(2)−C(2)	1.867(3)	O(4)−C(4)−Rh(4)	179.1(6)	O(4)−C(4)−Rh(4)	175.7(3)
Rh(3)−C(3)	1.895(6)	Rh(3)−C(3)	1.887(3)	O(51)−C(51)−Rh(5)	172.1(6)	O(51)−C(51)−Rh(5)	171.1(3)
Rh(4)−C(4)	1.886(6)	Rh(4)−C(4)	1.870(3)	O(52)−C(52)−Rh(5)	178.1(7)	O(52)−C(52)−Rh(5)	177.0(4)
Rh(5)−C(51)	1.925(7)	Rh(5)−C(51)	1.932(4)	O(53)−C(53)−Rh(5)	179.2(6)	O(53)−C(53)−Rh(5)	178.4(3)
Rh(5)−C(52)	1.927(7)	Rh(5)−C(52)	1.926(3)	O(12B)−C(12B)−Rh(2)	135.9(4)	O(12B)−C(12B)−Rh(1)	130.7(2)
Rh(5)−C(53)	1.915(7)	Rh(5)−C(53)	1.909(3)	O(12B)−C(12B)−Rh(1)	128.7(4)	O(12B)−C(12B)−Rh(2)	132.54(19)
Rh(1)−C(12B)	2.089(5)	Rh(1)−C(12B)	1.994(2)	O(14B)−C(14B)−Rh(4)	137.3(4)	O(14B)−C(14B)−Rh(4)	136.9(2)
Rh(2)−C(12B)	1.959(5)	Rh(2)−C(12B)	2.005(3)	O(14B)−C(14B)−Rh(1)	128.9(4)	O(14B)−C(14B)−Rh(1)	131.4(2)
Rh(1)−C(14B)	2.111(5)	Rh(1)−C(14B)	2.086(2)	O(23B)−C(23B)−Rh(3)	142.5(4)	O(23B)−C(23B)−Rh(3)	141.0(2)
Rh(4)−C(14B)	1.967(5)	Rh(4)−C(14B)	1.971(3)	O(23B)−C(23B)−Rh(2)	137.7(5)	O(23B)−C(23B)−Rh(2)	138.8(2)
Rh(2)−C(23B)	2.147(5)	Rh(2)−C(23B)	2.134(3)	O(24B)−C(24B)−Rh(2)	139.5(4)	O(24B)−C(24B)−Rh(2)	138.9(2)
Rh(3)−C(23B)	2.091(6)	Rh(3)−C(23B)	2.070(3)	O(24B)−C(24B)−Rh(4)	140.2(4)	O(24B)−C(24B)−Rh(4)	141.1(2)
Rh(2)−C(24B)	2.085(5)	Rh(2)−C(24B)	2.075(3)	O(34B)−C(34B)−Rh(3)	139.9(5)	O(34B)−C(34B)−Rh(3)	140.8(2)
Rh(4)−C(24B)	2.090(5)	Rh(4)−C(24B)	2.102(3)	O(34B)−C(34B)−Rh(4)	138.6(5)	O(34B)−C(34B)−Rh(4)	138.1(2)
Rh(3)−C(34B)	2.077(6)	Rh(3)−C(34B)	2.081(3)	O(35B)−C(35B)−Rh(3)	134.6(5)	O(35B)−C(35B)−Rh(3)	134.2(3)
Rh(4)−C(34B)	2.118(5)	Rh(4)−C(34B)	2.121(3)	O(35B)−C(35B)−Rh(5)	133.4(4)	O(35B)−C(35B)−Rh(5)	132.4(2)
Rh(3)−C(35B)	1.985(5)	Rh(3)−C(35B)	1.989(3)	Rh(2)−C(12B)−Rh(1)	95.4(2)	Rh(1)−C(12B)−Rh(2)	96.75(11)
Rh(5)−C(35B)	2.086(6)	Rh(5)−C(35B)	2.074(3)	Rh(4)−C(14B)−Rh(1)	93.8(2)	Rh(4)−C(14B)−Rh(1)	91.72(10)
C(11)−O(11)	1.124(6)	C(1)−O(1)	1.132(3)	Rh(3)−C(23B)−Rh(2)	79.8(2)	Rh(3)−C(23B)−Rh(2)	80.07(9)
C(12)−O(12)	1.116(6)			Rh(2)−C(24B)−Rh(4)	80.18(18)	Rh(2)−C(24B)−Rh(4)	79.89(10)
C(2)−O(2)	1.139(6)	C(2)−O(2)	1.135(3)	Rh(3)−C(34B)−Rh(4)	81.4(2)	Rh(3)−C(34B)−Rh(4)	81.03(9)
C(3)−O(3)	1.124(6)	C(3)−O(3)	1.142(3)	Rh(3)−C(35B)−Rh(5)	92.0(2)	Rh(3)−C(35B)−Rh(5)	93.37(12)
C(4)−O(4)	1.128(6)	C(4)−O(4)	1.138(3)	C(1N)−N−Rh(1)	117.3(3)	C(1N)−N(1)−Rh(1)	109.42(18)
C(51)−O(51)	1.138(7)	C(51)−O(51)	1.141(4)			C(2N)−N(2)−Rh(1)	108.98(17)
C(52)−O(52)	1.122(7)	C(52)−O(52)	1.140(4)	N−C(1N)−C(2N)	113.8(4)	C(2N)−C(1N)−N(1)	112.2(3)
C(53)−O(53)	1.148(7)	C(53)−O(53)	1.152(3)			C(1N)−C(2N)−N(2)	113.4(3)
C(12B)−O(12B)	1.191(5)	C(12B)−O(12B)	1.181(3)			N(1)−Rh(1)−N(2)	79.16(9)
C(14B)−O(14B)	1.166(5)	C(14B)−O(14B)	1.183(3)	C(1N)−C(2N)−C(2N)#1	112.4(5)		

[a] Symmetry transformations used to generate equivalent atoms: (#1) $-x+1, -y-1, -z+1$.

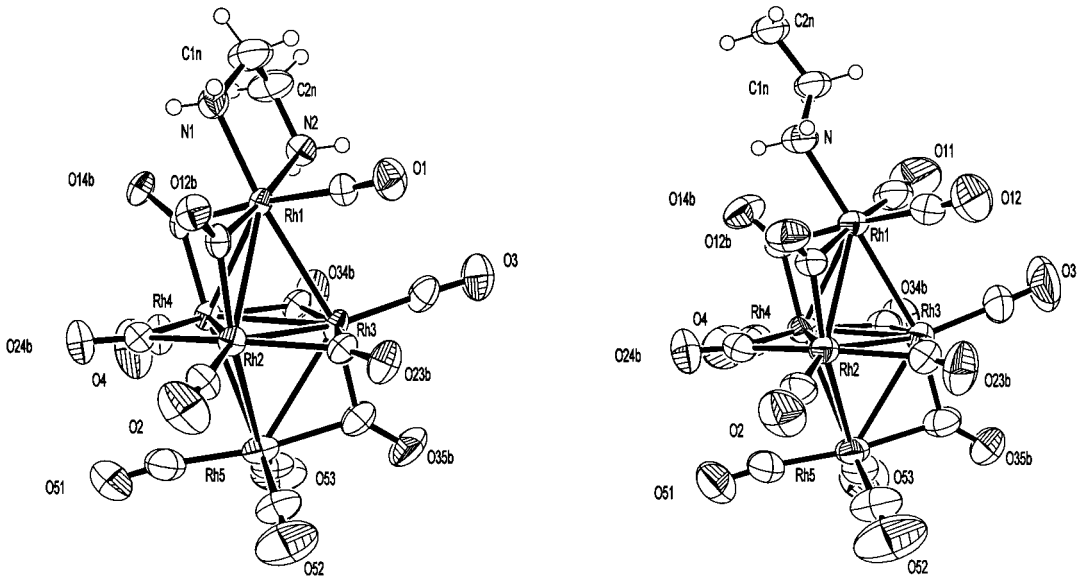

Figure 2. Comparative view of the two bipyramidal units of $[Rh_5(CO)_{13}(en)]^-$ (**2**, left) and $[Rh_5(CO)_{14}-(put)-Rh_5(CO)_{14}]^2$ (**1**, right). The C atoms of the carbonyl groups bear the same numbering as the respective connected O atoms. Ellipsoids are drawn at the 30% probability level. Hydrogen atoms have been drawn, for sake of simplicity, with arbitrary small *U* values.

The apical substituted Rh site has two "equatorial" positions (those trans to the two bridging COs) and one axial position (trans to the unsupported Rh1−Rh3 bond). In **1**, the putrescine ligand occupies the axial position (preserving

Table 4. Variable Temperature ^1H and ^{13}C NMR Spectra of $[Rh_5(CO)_{13}(en)]^-$ as $[PPN]^+$ Salt in THF-d_8 (δ in ppm; J_{Rh-C} in Hz; d = Doublet, t = Triplet)

	intensity	183 K	233 K	298 K
H (C1n)	2		2.60 (broad)	2.71
H (C2n)	2			2.49
H (N1,2)	1 + 1		1.63 + 2.33	1.84
	1 + 1		2.68 + 3.40	3.66
H (PPN)	30		7.3−7.9	7.3−7.7
C1n	1	43.17	44.10	44.65
C2n	1	48.34	47.23	46.32
C1	1	198.21 (d 57.5)	197.76 (d 58.0)	scrambles with C14b
C51, 52, 53	3	collapsed	199.00 (d 71.5)	scramble with C35b
C2, C4	1	199.33 (d 94.6)	199.52 (d 93.2)	199.14 (d 91.6)
	1	199.82 (d 92.5)		
C3	1	201.17 (d 93.6)	200.99 (d 93.8)	199.71 (d 90.7)
C12b	1	229.15 (t 31.0)	228.16 (t 33.7)	227.12 (t 34.5)
C14b	1	249.2 (dd 35.5, 24.9)	248.34 (dd 35.9−25.5)	scrambles with C1
C35b	1	253.55 (dd 31.6−31.1)	253.98 (dd 33.4−30.1)	scrambles with C51, 52, 53
C23b, C34b	2	259.44 (t ca. 30)	258.14 (t 32.2)	256.62 (t 33.0)
C24b	1	259.16 (t ca. 30)	259.33 (t 32.1)	258.99 (t 30.8)

the idealized C_s symmetry), while in **2**, the ethylenediamine ligand occupies the axial position and one equatorial site. The binding site common to both clusters could be considered the preferred one for a pure σ-donor. Accordingly, in **2**, the Rh−N_{axial} bond distance is shorter than the Rh−$N_{equatorial}$ (2.177(2) vs 2.222(2) Å). The amino ligand (a pure σ-donor) is markedly different from CO (a strong π-acceptor), and this allows for the shortening of the bonds trans to it. In particular, the unbridged Rh1−Rh3 in **1** and **2** is shorter than the average of the two bridged Rh1−Rh2 and Rh1−Rh4 bond distances (2.948 vs 2.987 Å for **1** and 2.936 vs 2.951 Å for **2**); analogously, Rh1−C12B in **2** is shorter than in **1** (1.994(2) vs 2.089(5) Å).

As far as steric effects are considered, the dimeric nature of **1** certainly favors the axial binding of the diamine since the putrescine length would not be sufficient to avoid repulsive interaction between the two pentametallic moieties if equatorially bound. On the other hand, it is doubtful whether a biequatorial stereoisomer of **2** would be more or less hindered than the observed one.

4. ^1H and ^{13}C NMR Spectra of (PPN)$[Rh_5(CO)_{13}(en)]$. The stability of $[Rh_5(CO)_{13}(en)]^-$ anion (**2**) allowed a detailed NMR study of its solution structure. ^1H and ^{13}C (natural abundance) NMR spectra have been obtained from its $[PPN]^+$ salt in THF-d_8. Some spectra, obtained under N_2, were re-collected after saturation of the solution with CO under a pressure of 1 atm at room temperature; the spectra remained unchanged with respect to those made under nitrogen, confirming the results of the IR spectra in that the carbon monoxide does not affect significantly the chelation of ethylenediamine. The results are summarized in Table 4.

In the solid-state structure of **2** the two carbon atoms of the chelating ethylenediamine ligand, C1n and C2n, are inequivalent and yield two distinct ^{13}C resonances (not absolutely assigned) whose spacing, ranging between 1.7 and 5.2 ppm, depends on the temperature. The effect is particularly relevant on C2n, which, as the temperature is lowered, moves ca. 2 ppm downfield. A heterocorrelate spectrum allowed the assignment of the resonances relative to the 2 + 2 hydrogen atoms on C1n and C2n at ca. 2.7 and 2.5 ppm, respectively.

The hydrogen atoms of the amino groups give very broad resonances centered, at room temperature, at 1.8 and 3.7 ppm (both of relative intensity 2). They are quite sensitive to the temperature and at ca. 233 K become split in four resonances of relative intensity 1, confirming that the asymmetric binding of the ligand is retained in solution.

The ^{13}C spectra in the carbonyl region change with the temperature because of fluxionality of the carbonyl ligands, as shown in Figure 3. The downfield triplet of relative intensity 2 has been assigned (with reference to the structure of Figure 2) to the two almost symmetry-equivalent C23b and C34b; it shows a remarkable temperature shift from 256.6 ppm (at 298 K) to 259.4 ppm (at 183 K), where it appears almost superimposed onto the triplet at ca. 259.2 ppm, labeled C24b. These assignments are consistent with those from previous NMR studies of heterometallic pentanuclear clusters,[17−19] where the edge-bridging carbonyls in the equatorial Rh_3 (or Ir_3) plane are not fluxional at room temperature and often yield triplets of intensity 2 + 1. The only other resonance that can be observed throughout the temperature range (183−298 K) is that assigned to C12b. Its anomalous location, considerably upfield with respect to the other resonances of bridging COs, suggests a somewhat higher electron density, as expected for the carbon trans to the N2 nitrogen ligand. Moreover, its expression as a triplet is in agreement with the solid-state structure that showed it as a nearly symmetric bridge. At lower temperatures (233 and 183 K), two other resonances of relative intensity 1 have been observed downfield; they are doublets of doublets, therefore consistent with the C14b and C35b that bridge asymmetrically the apical Rh atoms to the equatorial Rh_3 triangle. Our tentative assignment is based on the greater asymmetry of C14b that would yield a higher difference in the coupling constants (35.9 and 25.5 Hz) with respect C35b (33.4 and 30.1 Hz). The two signals are lost at room temperature.

Concerning the terminal CO region (around 200 ppm), several ^{13}C resonances are not observable at room temper-

(18) Fumagalli, A.; Martinengo, S.; Chini, P.; Galli, D.; Heaton, B. T.; Della Pergola, R. *Inorg. Chem.* **1984**, *23*, 2947.
(19) Fumagalli, A.; Della Pergola, R.; Bonacina, F.; Garlaschelli, L.; Moret, M.; Sironi, A. *J. Am. Chem. Soc.* **1989**, *111*, 165.

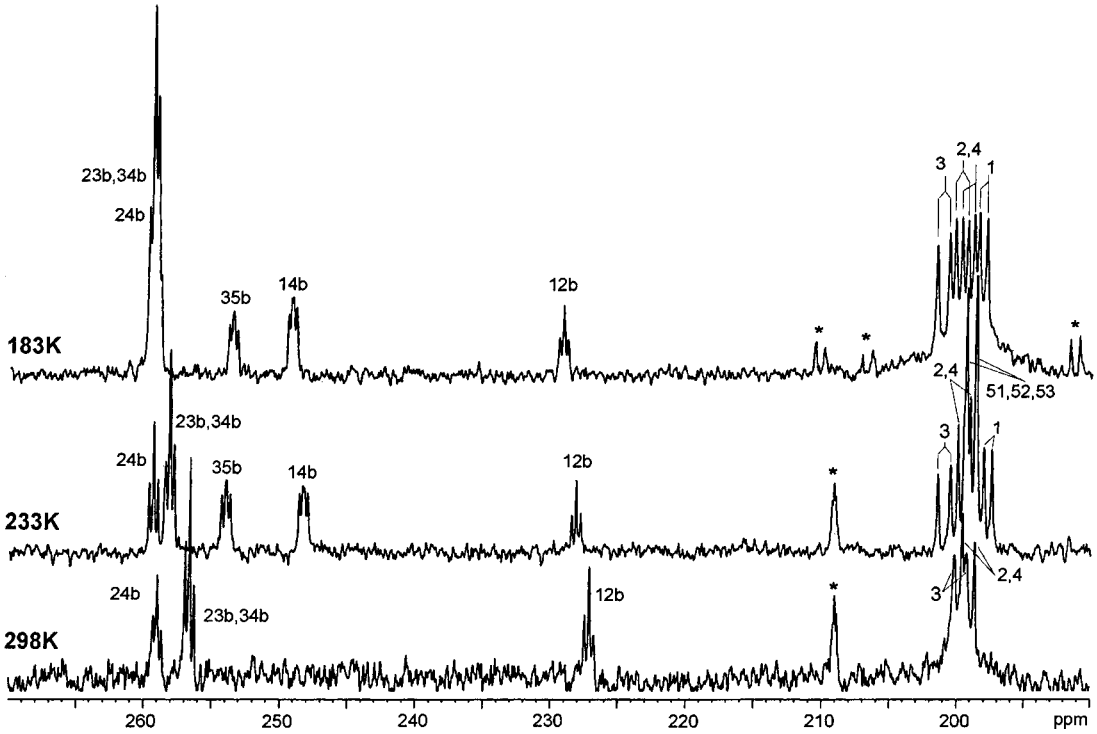

Figure 3. Variable-temperature ^{13}C NMR spectra of $[Rh_5(CO)_{13}(en)]^-$ as the $[PPN]^+$ salt in THF-d_8 at 183, 233, and 298 K (top to bottom). The carbon atoms are labeled with reference to Figure 2. The resonances marked ∗ are due to an impurity of $[Rh_6(CO)_{15}]^{2-}$ and account for less than 5%.

ature because of terminal−bridge exchange processes, which probably would reach coalescence at higher temperature. On the other hand, at 183 K (where all the bridges are fixed) the process of further differentiation of the terminally bound CO is still going on and a few ^{13}C resonances are still missing. Thus, the most revealing spectrum occurs at 233 K. At this temperature the seven terminal COs are grouped to give four doublets with relative intensities 1, 3, 2, and 1. The Rh−C distances (Table 3) were quite useful in assigning the labels; thus, the two signals at 197.76 ppm (intensity 1) and 199.0 ppm (intensity 3) can be easily related to the ligands bonded on the cluster apexes, respectively, on Rh1 and on Rh5. The Rh−C bonds are quite long, particularly those to C1 (with a J_{C-Rh} of only 58.0 Hz) and C51 (with an expected similar J_{C-Rh}); this latter is scrambling with C52 and C53 (expected J_{C-Rh} of 70−80 Hz), and the result is an averaged coupling of 71.5 Hz. These assignments match very well with previous assignments obtained with other pentanuclear $Rh_{5-x}M_x$ clusters. At lower temperatures C1 stays fixed, while C51, C52, and C53 are collapsed, on the way to become differentiated. Even at room temperature, the signals are lost, very likely because C1 is on the way to exchange with C14b while the three carbonyls on Rh5 begin to scramble with C35b.

A higher coupling constant (>90 Hz) characterizes, at room temperature and at 233 K, the two resonances labeled as C3 and C2 + C4 consistently with the short bonding distances. The two latter carbonyls cannot exchange with each other because of the fixed bridges; thus, the intensity 2 of the signal must arise from the superimposition of two resonances with very similar δ and J, in agreement with the similarity (but not equivalence) of the ligands in the solid-state structure. In fact, at 183 K, and this is quite remarkable, C2 and C4 appear differentiated (because they really are in the solid-state structure) and give two doublets at 199.3 and 199.8 ppm, whose baricenter almost coincides with the position of the resonance that originated them (199.5 ppm). The temperature shift of C3 is quite remarkable.

Finally, the peaks marked ∗ in the spectra of Figure 3 are due to an impurity. At 298 and 233 K there is just a resonance appearing as a septet at 209.0 ppm with J_{C-Rh} of ca. 13 Hz. This matches the results obtained for $[Rh_6(CO)_{15}]^{2-}$, which was reported fluxional from room temperature down to 203 K.[20] At 183 K, in our spectrum, three doublets with relative intensities of 1:2:2 become evident at 191.3 ppm (67 Hz), 206.8 ppm (75 Hz), and 210.2 ppm (79 Hz). The estimated molar fraction of the impurity is less than 0.05.

Conclusions

Two hypotheses may be proposed for the substitution mechanism of $[Rh_5(CO)_{15}]^-$. In one case, the first step would be a nucleophilic attack of the amine on a carbonylic carbon (possibly a terminal one for the greater positive polarization of the carbon), analogous to that suggested by Chini.[5] This intermediate, rather than evolving to a carbamoyl derivative (as in the reaction of the neutral carbonyl $Rh_6(CO)_{16}$), would eventually give an N−Rh bonding interaction as a CO is set free. However, we suggest (as more probable) that a substitution occurs going through a dissociative mechanism because the $[Rh_5(CO)_{15}]^-$ anion is known to reversibly lose CO to give eventually $[Rh_{12}(CO)_{30}]^{2-}$.[8,12,14] Thus, a two-step

(20) Heaton, B. T.; Towl, A. D. C.; Chini, P.; Fumagalli, A.; McCaffrey, D. J. A.; Martinengo, S. *J. Chem. Soc., Chem. Commun.* **1975**, 523.

sequence is postulated:

$$[Rh_5(CO)_{15}]^- \overset{-xCO}{\rightleftharpoons} [Rh_5(CO)_{15-x}]^- \xrightarrow{NH_2R} [Rh_5(CO)_{14}(NH_2R)]^- \quad (10)$$

The results obtained with the diamines with a rather long "spacer" suggest that in solution they are involved in a sequence of equilibria:

$$[Rh_5(CO)_{14}\text{-}n\text{—}n\text{-}Rh_5(CO)_{14}]^{2-} \rightleftharpoons$$

$$[\text{-}n\text{—}n\text{-}Rh_5(CO)_{14}]^- \rightleftharpoons [\begin{matrix} n \\ | \\ Rh_5(CO)_{13} \\ | \\ n \end{matrix}]^- \quad (11)$$

The main factors causing one binding mode to dominate over the others appear to be the concentration and the molar ratio ($n_2/[Rh_5(CO)_{15}]^-$) of the two reagents, the spacing between the two amino groups (i.e., the relative stability of the resulting ring as a function of its size), and a nitrogen atmosphere rather than a CO one. When the products have to be recovered, even the specific cation and the solvents play a critical role in shifting the equilibrium, since the differences in solubility between several anionic species present in solution may be greatly enhanced, thus favoring the selective precipitation of only one form (bulky cation salts of dianions are expectedly less soluble than those of monoanions). This was the case of the $\{[Rh_5(CO)_{14}]-(put)-[Rh_5(CO)_{14}]\}^{2-}$ dianion, which was isolated in crystalline form as the $[PPh_4]^+$ salt, probably with a lucky and perhaps unique combination of a cation with the right dimensions and of the opportune mixture of solvents. In fact, several attempts to isolate the $[PPN]^+$ salt of this putrescine derivative instead resulted in the precipitation of an amorphous impure solid along with some $[PPN][Rh_5(CO)_{15}]$.

Finally, the unexpected reactivity and the stability of these amino derivatives must be related to the peculiarity of $[Rh_5(CO)_{15}]^-$, particularly with respect to the two apexes that are the sites of the reaction. These metals should, if not positively polarized, at least have low electronic density. In this connection it must be recalled that an alternative interpretation of the metal−metal interactions has been proposed for the clusters having the geometry of an elongated trigonal bipyramid and 76 valence electrons (CVE), such as $[M_2Ni_3(CO)_{16}]^{2-}$ (M = Cr, Mo, W)[21] or $[PtIr_4(CO)_{14}]^{2-}$.[19] In these clusters the two apexes may be regarded as coordinatively unsaturated moieties (16 electrons) bonding both faces of an M_3 structure, a sort of cyclopropenyl ring able to donate 2 + 2 electrons.

Experimental Section

All operations were carried out under nitrogen or carbon monoxide where specified, with a standard Schlenk tube apparatus. Tetrahydrofuran was distilled from sodium benzophenone and 2-propanol from aluminum isopropoxide. All other analytical grade solvents were degassed in a vacuum and stored under nitrogen. $Rh_4(CO)_{12}$ [22] and $[Rh(CO)_4]^-$ (as the $[PPh_4]^+$ or $[N(PPh_3)_2]^+$ salt)[23] were prepared according to published methods. Infrared spectra were recorded on Perkin-Elmer 16PC or Nicolet Avatar 360 FT-IR spectrophotometers, using 0.1 mm CaF_2 cells previously purged with nitrogen. ^1H and ^{13}C NMR spectra were recorded with Bruker AC300 or Avance 400 spectrometers in THF-d_8 solvent as internal standard. ^{13}C NMR spectra were acquired using an inverse gated pulse sequence. 2D heterocorrelation (HETCOR) results were obtained with a 300 MHz instrument.

1. Synthesis of $[Rh_5(CO)_{15}]^-$. The synthesis of this anion was never reported in detail.[8,12]

1.a. $[PPN]^+$ Salt. In a typical preparation $[PPN][Rh(CO)_4]$ (3.264 g, 4.33 mmol) and $Rh_4(CO)_{12}$ (3.238 g, 4.33 mmol) were treated with THF (50 mL) under a CO atmosphere. After ca. 20 min of stirring, the resulting burgundy-red solution was checked for purity by its IR spectrum (2043s, 2010s, 1870m, 1841ms, and 1788ms cm^{-1}). The bands of $Rh_4(CO)_{12}$ (2074s and 1875ms cm^{-1}) and $[Rh(CO)_4]^-$ (1900s cm^{-1}) must not to be present; if this is the case, a correction may be done by addition of small amounts of one or the other reagent as required. The clear solution was then carefully layered with 2-propanol (160 mL, previously saturated with CO). When the diffusion of the solvents was complete (about a week), the mother liquor was syringed off and the dark-red crystals were quickly vacuum-dried and stored under a CO atmosphere. Yields: better than 80%.

1.b. $[PPh_4]^+$ Salt. This salt cannot be isolated in a crystalline form but can be prepared and maintained in solution where it is indefinitely stable under 1 atm of CO. Thus, equimolecular amounts of $Rh_4(CO)_{12}$ and $(PPh_4)[Rh(CO)_4]$ (up to 1.5 mmol, respectively) were dissolved with stirring in THF (typically 20 mL) under 1 atm of CO to yield the burgundy-red solution of known concentration, which was used entirely or in portions as required, for the following preparations of the $[PPh_4]^+$ salts.

2. Synthesis of $\{[Rh_5(CO)_{14}]-NH_2(CH_2)_4H_2N-[Rh_5(CO)_{14}]\}^{2-}$ (1). 2.a. $[PPh_4]^+$ Salt. $[PPh_4][Rh_5(CO)_{15}]$ was obtained in solution by reaction of $[PPh_4][Rh(CO)_4]$ (281 mg, 0.507 mmol) with $Rh_4(CO)_{12}$ (379 mg, 0.507 mmol) in THF (5 mL) under 1 atm of CO. An excess of putrescine (70 mg, 0.794 mmol) was then added, while stirring. The sudden change of color (from burgundy-red to orange) and the bubbling of evolved CO gave evidence of reaction. An IR spectrum revealed presence of both the chelate and monodentate forms. The solution was cautiously layered with a mixture of 2-propanol and *n*-hexane (2:1, 45 mL) previously saturated with CO. The product was recovered after ca. 1 month as orange crystals. Yield: 570 mg, 87%. Anal. Found (calcd) for $C_{80}H_{52}N_2O_{28}P_2Rh_{10}$: C, 38.80 (37.24); H, 2.33 (2.03); N, 1.81 (1.09). The reported structure was obtained from this salt. The IR spectrum of the crystals in Nujol mull is that reported in Table 1; the IR spectrum in THF solution gave evidence of essentially the monodentate form in a mixture with minor amounts of $[Rh_5(CO)_{15}]^-$ and traces of the chelate form.

2.b. $[PPN]^+$ Salt. The product was prepared similarly starting from $[PPN][Rh_5(CO)_{15}]$ but resulted as an orange amorphous solid, impure with some $[PPN][Rh_5(CO)_{15}]$. Anal. Found (calcd) for $C_{104}H_{72}N_4O_{28}P_4Rh_{10}$: C, 39.31 (41.94); H, 2.61 (2.44); N, 1.14 (1.88).

3. Synthesis of $[Rh_5(CO)_{13}(n_2)]^-$ for n_2 = en, R-1,2-prn, or 1,3prn. 3.a. $[Rh_5(CO)_{13}(en)]^-$ (2) as $[PPN]^+$ or $[PPh_4]^+$ Salt. $[PPN][Rh_5(CO)_{15}]$ (660 mg, 0.448 mmol) was dissolved in THF

(21) Ruff, J. K.; White, R. P.; Dahl, L. F. *J. Am. Chem. Soc.* **1971**, *93*, 2159.

(22) Martinengo, S.; Giordano, G.; Chini, P. *Inorg. Synth.* **1980**, *20*, 209.

(23) Garlaschelli, L.; Della Pergola, R.; Martinengo, S. *Inorg. Synth.* **1991**, *28*, 211.

Table 5. Crystal Data and Structure Refinement for $[Rh_5(CO)_{14}-(put)-Rh_5(CO)_{14}][PPh_4]_2$ and $[Rh_5(CO)_{13}(en)][PPh_4]\cdot THF$[a]

empirical formula	$C_{92}H_{76}N_2O_{31}P_2Rh_{10}$	$C_{43}H_{36}N_2O_{14}PRh_5$
fw	2796.59	1350.26
temp (K)	298(2)	233(2)
wavelength (Å)	0.710 73	0.710 73
cryst system, space group	monoclinic	triclinic
space group	$P2/n$	$P\bar{1}$
a (Å)	23.209(3)	11.999(2)
b (Å)	9.8300(10)	12.760(2)
c (Å)	23.683(3)	16.919(2)
α (deg)	90	99.940(10)
β (deg)	110.230(10)	101.400(10)
γ (deg)	90	106.300(10)
vol (Å^3)	5069.8(11)	2364.5(6)
Z	2	2
calcd density (Mg/m^3)	1.832	1.896
abs coeff (mm^{-1})	1.691	1.808
F(000)	2740	1320
cryst size (mm)	0.20 × 0.15 × 0.10	0.25 × 0.15 × 0.10
θ range for data collection (deg)	1.52−29.30	1.27−29.24
limiting indices	$-31 \le h \le 29$, $0 \le k \le 13$, $0 \le l \le 31$	$-16 \le h \le 16$, $-16 \le k \le 16$, $-22 \le l \le 22$
reflns collected/unique	58994/12830 [R(int) = 0.019, R_σ = 0.058]	27376/11515 [R(int) = 0.0265, R_σ = 0.0487]
completeness to θ = 29.24 (%)	92.4	89.3
max and min transm	0.8491 and 0.7285	0.8399 and 0.6607
refinement method	full-matrix least-squares on F^2	full-matrix least-squares on F^2
data/restraints/params	12830 / 0 / 550	11515 / 0 / 602
GOF on F^2	0.972	0.842
final R indices [$I > 2\,\sigma(I)$]	R1 = 0.0492, wR2 = 0.0833	R1 = 0.0229, wR2 = 0.0434
R indices (all data)	R1 = 0.0993, wR2 = 0.0944	R1 = 0.0388, wR2 = 0.0450
largest diff peak and hole (e Å^{-3})	0.580 and −0.471	0.789 and −0.644

[a] $R_{int} = \sum|F_o^2 - F_{mean}^2|/\sum F_o^2$; $R_\sigma = \sum\sigma(F_o^2)/\sum F_o^2$; $R1 = \sum||F_o| - |F_c||/\sum|F_o|$; $wR2 = (\sum(F_o^2 - F_c^2)^2/\sum wF_o^4)^{1/2}$.

(10 mL) under a CO atmosphere and, while stirring, treated with ethylenediamine (31 μL, ca. 0.46 mmol). The immediate change of color from burgundy-red to orange-yellow and the conspicuous gas evolution are indicative of the reaction, which the IR spectrum confirms to be complete. After a couple of hours of stirring, if there is evident precipitation of some impurities, filtration may be required. The clear solution is then cautiously layered with 2-propanol (70 mL) previously saturated with CO. After a couple of weeks, at the end of the diffusion, the mother liquor was removed with a syringe, leaving an amorphous orange precipitate. This was twice washed with 2-propanol (10 mL), decanted, and separated from the washings. After a short vacuum-drying, the product was stored under CO. Yield: ca. 500 mg, 80%. Anal. Found (calcd) for $C_{51}H_{38}N_3O_{13}P_2Rh_5$: C, 40.95 (41.46); H, 2.59 (2.59); N, 2.83 (2.84). IR data are in Table 1. The NMR spectra reported above were done on this salt.

The $[PPh_4]^+$ salt was done using an appropriate portion of the solution prepared in **1b** with ca. 10−20% excess of ethylenediamine. Crystallization was done similarly with cautious layering of 2-propanol previously saturated with CO. The orange crystals of $[PPh_4][Rh_5(CO)_{13}(en)]\cdot THF$ obtained in this way were suitable for the reported X-ray crystal structure determination.

3.b. [PPN][Rh$_5$(CO)$_{13}$(*R*-1,2prn)]. The reaction was done as for **3a** with $[PPN][Rh_5(CO)_{15}]$ (382 mg, 0.259 mmol) and (*R*)-(+)-1,2-diaminopropane (57 mg, 0.380 mmol) in 5 mL of THF. Crystallization was made by cautious layering of a mixture of 2-propanol and *n*-hexane (2:1, 20 mL) previously saturated with CO. The orange crystals obtained were mixed with a black laque. A sample of hand-picked crystals gave the IR data reported in Table 2 and the following analysis. Anal. Found (calcd) for $C_{52}H_{40}N_3O_{13}P_2Rh_5$: C, 42.66 (41.88); H, 2.92 (2.70); N, 2.73 (2.88).

3.c. [PPN][Rh$_5$(CO)$_{13}$(1,3prn)]. The reaction was done as for **3a** with $[PPN][Rh_5(CO)_{15}]$ (378.6 mg, 0.257 mmol) and 1,3 diaminopropane (30 μL, ca. 0.35 mmol) in 5 mL of THF. Crystallization was made by cautious layering of a mixture of 2-propanol and *n*-hexane (2:1, 20 mL) previously saturated with CO to yield orange crystals mixed with some dark amorphous material. A few hand-picked crystals gave the reported IR data (Table 2) and the following analysis. Anal. Found (calcd) for $C_{52}H_{40}N_3O_{13}P_2Rh_5$: C, 41.80 (41.88); H, 2.83 (2.70); N, 3.21 (2.882).

4. Reaction of [Rh$_5$(CO)$_{15}$]$^-$ with Amines and Diamines That Did Not Yield Isolable Products. In the following procedures we could observe the substitution reaction, but the products were not isolated.

4.a. 1,5-Diaminopentane. $[N(PPh_3)_2][Rh_5(CO)_{15}]$ (758 mg, 0.515 mmol) was dissolved in 5 mL of THF under CO and treated with 1,5-diaminopentane (61 mg, 0.6 mmol), causing the characteristic change of color (from red to orange) and gas evolution. After 30 min of stirring of the solution, whose IR was indicative of monosubstitution (Table 1), the solution was decanted and cautiously layered with a 2:1 mixture of 2-propanol and *n*-hexane (20 mL) previously saturated with CO. When the diffusion was complete, the recovered product revealed decomposition. Several other attempts at crystallization, by changing the cation ($[NEt_4]^+$, $[PPh_4]^+$) and the solvents, gave similar decomposition.

4.b. Benzylamine. $[N(PPh_3)_2][Rh_5(CO)_{15}]$ (207.5 mg, 0.141 mmol) was dissolved in 5 mL of THF and was treated with benzylamine (18 μL, ca. 0.165 mmol), causing the characteristic change of color (from red to orange) and gas evolution. The IR spectrum is reported in Table 1 and is consistent with monosubstitution. Major decomposition occurred during the crystallization attempts.

4.c. 3-Phenylpropylamine. A reaction was done similarly to the one reported for **4b** with near-stoichiometric amounts of 3-phenylpropylamine. The solution IR spectrum is reported in Table 1. Crystallization attempts gave decomposition.

4.d. Piperidine. $[N(PPh_3)_2][Rh_5(CO)_{15}]$ (160 mg, 0.109 mmol) was dissolved in 7 mL of THF and was treated with piperidine (20 μL, ca. 0.200 mmol). The reaction ran as usual with a change of

color and gas evolution to yield the IR spectrum reported in Table 1. Any attempt at crystallization failed.

5. X-ray Structure Determinations of $[PPh_4]_2[Rh_5(CO)_{14}-(put)-Rh_5(CO)_{14}]$ and $[PPh_4][Rh_5(CO)_{13}(en)]\cdot THF$. X-ray data were measured for two suitable crystals of the title compounds with a Siemens SMART CCD area detector diffractometer. Crystal data are presented in Table 5. Graphite-monochromatized Mo Kα (λ = 0.710 73 Å) radiation was used with the generator at 45 kV and 40 mA. Initial cell parameters and orientation matrix were obtained from least-squares refinement on reflections measured in three different sets of 15 frames each. For both crystals a full sphere was sampled (2100 frames; sample−detector distance 5 cm; 20 s per frame; $\Delta\omega = 0.3°$). The first 100 frames were re-collected to have a monitoring of any crystal decay, which was not observed. An empirical absorption correction was applied (SADABS[24]). The structures were solved by direct methods (SIR97[25]) and refined with full-matrix-block least squares (SHELX97[26]). Anisotropic temperature factors were assigned to all non-hydrogenic atoms. Hydrogen atoms were positioned at idealized locations.

Acknowledgment. This paper is dedicated to our colleague and friend Secondo Martinengo in the second anniversary of his untimely death. With his amiable character and unique practical skill, he introduced most of us to cluster chemistry.

Supporting Information Available: One X-ray crystallographic file, in CIF format, and Figure 1S showing the IR spectra of $[Rh_5(CO)_{13}(put)]^-$, $[Rh_5(CO)_{14}-(put)-Rh_5(CO)_{14}]^{2-}$, and their mixture as obtained under CO. This material is available free of charge via the Internet at http://pubs.acs.org.

IC0107936

(24) Sheldrick, G. M. *SADABS*; University of Göttingen: Göttingen, Germany, 1996.

(25) Altomare, A.; Cascarano, G.; Giacovazzo, C.; Guagliardi, A.; Burla, M. C.; Polidori, G.; Camalli, M. *J. Appl. Crystallogr*. **1994**, *24*, 435.

(26) Sheldrick, G. M. *SHELX97—Program for the Refinement of Crystal Structure;* University of Göttingen: Göttingen, Germany.